Author Manuscript

Author Manuscript

Author Manuscript

Author Manuscript

HHS Public Access

Author manuscript

Hippocampus. Author manuscript; available in PMC 2019 January 01.

Published in final edited form as:

Hippocampus. 2019 January ; 29(1): 26–36. doi:10.1002/hipo.23026.

Task-Enhanced Arterial Spin Labeled Perfusion MRI Predicts Longitudinal Neurodegeneration in Mild Cognitive Impairment

Long Xie[a], **Sandhitsu R. Das**[a,c,d], **Arun Pilania**[c,d], **Molly Daffner**[c,d], **Grace E. Stockbower**[c,d], **Sudipto Dolui**[b,d,e], **Paul A. Yushkevich**[a,e], **John A. Detre**[b,d,e], and **David A. Wolk**[c,d]

[a]Penn Image Computing and Science Laboratory (PICSL), Department of Radiology, University of Pennsylvania, Philadelphia, PA, USA

[b]Center for Functional Neuroimaging, Department of Neurology, Department of Radiology, University of Pennsylvania, Philadelphia, PA, USA

[c]Penn Memory Center, University of Pennsylvania, Philadelphia, PA, USA

[d]Department of Neurology, University of Pennsylvania, Philadelphia, PA, USA

[e]Department of Radiology, University of Pennsylvania, Philadelphia, PA, USA

Abstract

Mild cognitive impairment (MCI) is considered a prodromal stage of Alzheimer's disease (AD), but is also recognized to be a heterogeneous condition. Biomarkers that predict AD progression in MCI are of clinical significance because they can be used better identify appropriate candidates for therapeutic intervention studies. It has been hypothesized that, comparing to structural measurements, functional ones maybe more sensitive to early disease abnormalities and the sensitivity could be further enhanced when combined with cognitive task, a "brain stress test". In this study, we investigated the value of regional cerebral blood flow (CBF), measured by arterial spin labeled perfusion MRI (ASL MRI) during a memory-encoding task, in predicting the estimated rate of hippocampal atrophy, an established marker of AD progression. Thirty-one amnestic MCI patients (20 male and 11 female; age: 70.9 ± 6.5 years, range from 56 to 83 years; mini mental status examination: 27.8 ± 1.8) and 42 normal control subjects (13 male and 29 female; age: 70.6 ± 8.8 years, range from 55 to 88 years; mini mental status examination: 29.1 ± 1.2) were included in this study. We compared the predictive value of CBF during task to CBF during rest and structural volumetry. Both region-of-interest and voxelwise analyses showed that baseline CBF measurements during task (strongest effect in fusiform gyrus, region-of-interest analysis statistics: $r = 0.56$, $p = 0.003$), but not resting ASL MRI or structural volumetry, were correlated with the estimated rate of hippocampal atrophy in amnestic MCI patients. Further, stepwise linear regression demonstrated that resting ASL MRI and volumetry did not provide complementary information in prediction. These results support the notion that physiologic measures during a cognitive challenge may increase the ability to detect subtle functional changes

Corresponding to: Long Xie, Penn Image Computing and Science Laboratory (PICSL), 3700 Hamiton Walk, Richards building 6th floor, Philadelphia, PA 19104, USA, lxie@seas.upenn.edu.

Conflict of interests:

Dr. Wolk received grants from Eli Lilly/Avid Radiopharmaceuticals, personal fees from Eli Lilly, grants and personal fees from Merck, grants from Biogen, personal fees from Janssen, and personal fees from GE Healthcare.

Author Manuscript Author Manuscript Author Manuscript Author Manuscript

that predict progression. As such, ASL MRI could have important utility in stratifying candidates for AD treatment trials.

Keywords

Alzheimer's disease; ASL MRI; biomarker; longitudinal neurodegeneration; mild cognitive impairment

1. Introduction

One of the central goals of Alzheimer's disease (AD) research is the development of therapeutic interventions to prevent or delay disease progression. Mild cognitive impairment (MCI) is often the prodromal stage of AD (Jack et al., 2013), and patients with this condition are commonly targeted for therapeutic intervention studies or clinical trials (Sevigny et al., 2016). However, MCI is a heterogeneous condition comprised of patients with a variety of clinical outcomes (Petersen et al., 2001). Cognitive symptoms in a significant proportion of MCI patients may remain stable for long periods of time, or even improve, and some do not progress to AD or other forms of dementia when followed longitudinally (Petersen, 2016). Even amongst those who are destined to develop AD, rates of progression can vary significantly (Dickerson and Wolk, 2013; Petersen, 2016). While a number of biomarkers can indicate AD risk or track AD progression, baseline measurements that can identify MCI patients who are likely to progress within a particular timeframe would be extremely valuable both for patient selection or stratification in therapeutic trials and clinically as prognostic indicators.

It has been hypothesized that, subtle synaptic abnormalities may precede neuronal death in the early stages of AD (Small, 2005). Hence, measurements of brain function may be particularly sensitive to early effects of disease pathophysiology relative to measures of brain structure (Wang, 2014). Arterial spin labeled perfusion magnetic resonance imaging (ASL MRI) can be used to quantify regional cerebral blood flow (CBF), which is thought to be tightly coupled to brain metabolism, that, in turn, is linked to synaptic activity (Raichle, 1998).

The first aim of the current study is to explore the value of ASL MRI in predicting disease progression in the prodromal stage of AD. In recent years, ASL MRI has been increasingly studied in the context of AD (Alsop et al., 2000; Dai et al., 2009; Chen et al., 2011b; Wang et al., 2013; Wolk and Detre, 2012), including work suggesting that alterations of perfusion may precede that of other functional, structural, and molecular biomarkers (Iturria-Medina et al., 2016). A number of studies have supported its potential utility in detecting abnormalities at prodromal and even preclinical disease stages (Binnewijzend et al., 2013; Toma, 2015; Dolui et al., 2017a; Sierra-Marcos, 2017). However, there is much more limited work in its ability to predict longitudinal outcomes related to disease progression. So far, only one longitudinal study of MCI patients has been conducted by Chao and her colleagues (Chao et al., 2010). They reported that hypoperfusion in right precuneus, inferior parietal, middle cingulum and middle frontal gyrus were associated with conversion from MCI to AD and cognitive decline (Chao et al., 2010). However, their implementation of ASL MRI did not

Author Manuscript Author Manuscript Author Manuscript Author Manuscript

cover the inferior part of the brain including the medial temporal lobe. Since the medial temporal lobe cortices and hippocampus are the earliest regions affected by AD neurofibrillary tangle pathology (Braak and Braak, 1995), baseline perfusion measurements in those regions could potentially have stronger predictive power of disease progression.

The notion that a task paradigm might serve as a “brain stress test” to enhance the sensitivity of functional measurements to early abnormalities has been widely explored in AD using task-related blood oxygen level dependent functional magnetic resonance imaging (BOLD fMRI). Although numerous BOLD fMRI studies have demonstrated task activation differences between AD, MCI and controls, only a few have assessed the utility of BOLD fMRI task activation in predicting longitudinal outcomes related to disease progression in MCI patients. To the best of our knowledge, only six have reported that baseline fMRI activation is predictive of cognitive decline in MCI (Miller et al., 2007; Petrella et al., 2007; Vannini et al., 2007; O’Brien et al., 2010; Kochan et al., 2011; Huijbers et al., 2015). Although BOLD fMRI provides a powerful approach for mapping brain function, a limitation of BOLD fMRI is that brain activity is measured indirectly through the effects of regional deoxyhemoglobin changes on regional magnetic susceptibility, precluding absolute quantification of either resting regional brain activity or changes in regional brain activity in response to a task. In contrast, ASL MRI allows quantification of brain activity in both resting and task states, as manifested in regional CBF.

The second aim of the current study is to determine the relative predictive power of resting versus task-enhanced ASL MRI. Xu et al. were the first to assess the effects of task activation using a memory-encoding paradigm on CBF in amnestic MCI patients (Xu et al., 2007). They confirmed decrements in resting perfusion, but even greater relative hypoperfusion during task for MCI relative to control subjects. We similarly demonstrated that ASL MRI acquired during the performance of a relatively short (~6 min) visual scene-encoding task displayed stronger discrimination of amnestic MCI (a-MCI) patients from cognitively normal adults than CBF obtained at rest, and provided complementary prediction to traditional structural MRI measures (i.e. hippocampal volume) (Xie et al., 2016). Hippocampal volume is the most well-studied neuroimaging AD biomarker and longitudinal volume change in this structure has been shown to be associated with AD progression in a number of studies (Chételat et al., 2005; Eckerström et al., 2008; den Heijer et al., 2010; Leung et al., 2013).

To summarize, the objectives of the current study were twofold. First, we compared the predictive power for evidence of progressive neurodegeneration (i.e. hippocampal volume change) of CBF measurements to other commonly used structural biomarkers derived from volumetric MRI. Second, we wanted to determine the relative value of regional CBF, measured by ASL MRI both during performance of a visual scene memory-encoding task and at rest in predicting hippocampal volume change. In order to achieve this, correlation analyses were performed between estimated hippocampal atrophy rate with structural measurements and CBF measurements during task/rest in *a priori* selected regions-of-interest that have previously been associated with MCI and early AD. Voxelwise correlation analyses were also performed to explore further brain areas in which baseline measurements show significant predictive power. In addition to validating regional CBF as a predictor of

Author Manuscript Author Manuscript Author Manuscript Author Manuscript

neurodegeneration in AD, these analyses provide insight into the relationship between baseline brain function and structural changes.

2. Materials and methods

2.1. Participants

Thirty-one a-MCI patients and 42 normal control (NC) subjects were recruited from the Penn Memory Center with a baseline and at least one follow-up visit. The a-MCI patients were recruited from a clinical sample, while the NCs were recruited from the community. A number of standardized psychometric assessments (items listed in Table 1) were performed as part of the evaluation at both time points. Clinical diagnosis of a-MCI was determined in a consensus conference attended by neurologists, psychiatrists, geriatricians, and neuropsychologists and followed the criteria outlined by Petersen and others (Petersen, 2004; Winblad et al., 2004; Petersen et al., 2009). Exclusion criteria include history of clinical stroke, significant traumatic brain injury, alcohol or drug abuse/dependence, or any other medical or psychiatric condition thought to significantly impact cognition. The study was approved by the Institutional Review Board of the University of Pennsylvania.

2.2 MRI acquisition

A 3T Siemens Trio MRI scanner (Erlangen, Germany), with either a product 8-channel or 32-channel array coil, was used to acquire structural images [three-dimension magnetization-prepared rapid gradient-echo (MPRAGE) (Mugler and Brookeman, 1990), inversion time/echo time/repetition time = 950ms/3ms/1620ms] and ASL MRI scans [pseudo-continuous ASL (pCASL) (Wu et al., 2007; Dai et al., 2008) acquired using two-dimension gradient-echo echo planar imaging (GR-EPI), repetition time/echo time/flip angle = 4s/19ms/90°, 6mm slice thickness, 1.2mm inter-slice gap, 16 slices acquired in ascending order, $3.5\times3.5mm^2$ in-plane resolution, 1.5s labeling duration, 1.5s post-labeling delay] at the baseline time point. Two perfusion scan sessions (about 6 min each) were performed while the subject was at ‘rest’ and performing a visual scene-encoding memory task (detail in Section 2.3). Due to technical or logistical issues, baseline “task” scans from 4 subjects (3 NC, 1 a-MCI) were not obtained. In the follow-up time point, clinical assessment and the MRI protocol were repeated.

2.3 Visual scene-encoding memory task

The visual scene-encoding memory task was described in prior studies (Fernández-Seara et al., 2007; Mechanic-Hamilton et al., 2009; Xie et al., 2016) and is summarized in brief in the following. Before the perfusion scan session, subjects were instructed to remember 72 complex real-world scenes selected from Photodisc photographic archive (Photodisc, Inc., Seattle, WA, USA). During the session (6 minutes), the 72 images were divided in three blocks (‘task’ blocks of 24 images) with each image presented for 3500ms with a 500ms interstimulus interval. Three short ‘rest’ blocks were interposed between ‘task’ blocks, in which 6 pixelated, unrecognizable images with randomly positioned shaded ‘X’ or ‘T’ were shown and presented with a 500ms interstimulus interval. To ensure the focus of the subject and to enhance ‘deep’ semantic encoding, subjects needed to make a subjective judgment about the meaningfulness of the images during ‘task’ blocks and identify the letter ‘X’/’T’

Author Manuscript Author Manuscript Author Manuscript Author Manuscript

during ‘rest’ blocks by button press. Immediately after the scanning session, a recognition memory test was performed. Participants were instructed to identify the studied images from 40 images (20 studied, 20 unstudied). An outcome measure, d-prime (d’), was computed in a standard fashion based on signal detection theory (Snodgrass and Corwin, 1988).

2.4 Neuroimaging data processing

2.4.1 Quantification of structural and functional measurements at baseline

Normalized hippocampal volume estimation: Each subject’s bilateral hippocampi were automatically segmented from the baseline anatomical MRI scan using a multi-atlas label fusion technique described in (Wang et al., 2012). The average bilateral hippocampal volume was then computed and normalized by intracranial volume [ICV, computed from the brain mask generated from FSL Brain Extraction Tool (BET) (Smith, 2002)] using equation (1).

$$Normalized\_HippoVolume = \frac{Whole\_Cohort\_Mean\_ICV}{Subject\_ICV} \times Subject\_HippoVolume \quad (1)$$

Cortical thickness estimation: he cortical thickness analysis pipeline (Das et al., 2009) available in Advanced Normalization Tools (ANTs, http://stnava.github.io/ANTs) was applied to the baseline anatomical MRI scans. It outputs a voxel-wise cortical thickness map for each subject.

Cerebral blood flow quantification: CBF maps were quantified from ASL MRI scans using Statistical Parametric Mapping 8 (SPM 8, Wellcome Department of Cognitive Neurology, UK), ASLtbx (a SPM add-on toolbox) (Wang et al., 2008) and Structural Correlation-based Outlier Rejection (SCORE) denoising algorithm (Dolui et al., 2017b). Visual inspection was performed to exclude subjects with CBF maps that have extensive non-physiological negative CBF clusters in gray matter, probably due to motion, other sources of MRI artifacts or instability of spin labeling. In total, resting CBF maps from 2 subjects (1 NC, 1 a-MCI) and task CBF maps from 4 (3 NC, 1 a-MCI) subjects were excluded from the study.

2.4.2 Longitudinal hippocampal atrophy rate estimation—

Automatic Longitudinal Hippocampal Atrophy software/package (ALOHA) (Das et al., 2012) was applied to generate unbiased estimation of hippocampal atrophy rate. The pipeline takes the structural scans of the two time points and the hippocampal segmentation in the baseline (generated in Section 2.4.1) as inputs and outputs the longitudinal hippocampal atrophy estimation [$(Volume_{Follwup} - Volume_{Basline})/Volume_{Basline}$]. The hippocampal atrophy was annualized [dividing it by the time difference between the two MRI scans (mean: 1.35 ± 0.33 years)] to compute the estimated rate of hippocampal atrophy. Due to severe MRI distortion and low signal-to-noise ratio, the atrophy rate measurements of 3 subjects (1 NC, 2 a-MCI) appeared unusable and they were excluded from the study.

Author Manuscript Author Manuscript Author Manuscript Author Manuscript

2.5 Longitudinal neuropsychological test data processing

For each neuropsychological test, we first subtract the score at the baseline time point from that of the followup. The difference was then annualized by dividing it by the time difference between the dates that the two tests were conducted (mean: 1.37 ± 0.40 years). To maintain consistency for the sign of longitudinal measurements [negative always indicating a change in a worse direction, e.g. greater estimated rate of hippocampal atrophy or decline of Mini Mental Status Examination (MMSE) score], we flipped the signs of the Trail A and Trail B, which are measured as a duration with longer meaning worse performance.

2.6 Statistical analysis

Analysis for demographic and neuropsychological data: To test the difference of demographic, neuropsychological test results at baseline and their longitudinal change between a-MCI and NC, contingency χ^2 test (sex) and independent two-sample t-tests (the rest of the measures) were performed. The above tests, along with the other statistical analyses in this paper, are two-sided with significance levels of $p = 0.05$ unless stated otherwise.

Region of interest (ROI) analysis: The relationship between neuroimaging-derived structural and functional measurements and the estimated rate of hippocampal atrophy was first investigated at a ROI level. The *a priori* selected ROIs include posterior cingulate cortex (PCC), precuneus, parahippocampal gyrus and fusiform gyrus derived from the Anatomical Automatic Labeling (AAL) template (Tzourio-Mazoyer et al., 2002) and the hippocampus generated in Section 2.3.1. All of these regions have been consistently reported to be involved in early AD (Petrie et al., 2009; Filippini et al., 2011), are often associated with memory function, and represent nodes of the default mode network. Moreover, these are regions that previously displayed sensitivity to task performance and discrimination between MCI and NC adults (Xie et al., 2016). The mean cortical thickness (for hippocampus ROI, we used volume), resting CBF and task CBF measurements of each ROI were derived by averaging values within gray matter voxels in that ROI. Bilateral structural (cortical thickness/hippocampal volume) and functional (resting and task CBF) measurements of each ROI were averaged. In addition, to investigate potential global effects, the mean structural and functional measurements in all cortical gray matter were also extracted. Partial correlation analyses, controlling for age, were performed between the estimated rate of hippocampal atrophy and each of the above neuroimaging-derived ROI measurement at baseline for the a-MCI and NC subjects separately. For the whole cohort, sex was included as an additional covariate due to the unmatched sex ratio between a-MCI and NC. Bonferroni correction was used to correct for multiple comparisons. To further investigate whether the different measurements provide complementary information in predicting the estimated rate of hippocampal atrophy, we performed a two-step, hierarchical linear regression with age (for a-MCI and NC, sex was included as an additional covariate for the whole cohort) entered in the first step and then task CBF, resting CBF and structural measurements included in the second step in a step-wise manner. In this analysis, only subjects with all the measurements available were included in the model. In addition, similar analyses were also performed with longitudinal rate of MMSE change as the dependent variable.

Author Manuscript Author Manuscript Author Manuscript Author Manuscript

Voxel-wise analysis: In addition to ROI analysis, we also performed voxel-wise analyses to further explore the regions in the brain that predict the estimated hippocampal atrophy rate. The resting CBF maps, task CBF maps and the voxelwise cortical thickness maps were normalized to the Montreal Neurological Institute (MNI) template space (template resolution: 1.0×1.0×1.0 mm^3 for thickness maps, 2.0×2.0×2.0 mm^3 for CBF maps). These normalized maps were entered into a whole brain voxel-wise general linear modal with hippocampal volume change as the dependent variable, resting/task CBF or cortical thickness at each gray matter voxel as independent variable and age as covariate (for a-MCI and NC, sex was included as an additional covariate for the whole cohort). The raw maps of t-statistic were enhanced by threshold-free cluster enhancement (TFCE) (Smith and Nichols, 2009) available in the FSL "randomise" package (Winkler et al., 2014). Permutation testing with 5,000 iterations were used to convert the TFCE-enhanced statistical maps to voxel-wise corrected *p*-values [using family-wise error rate (FWE) correction (Nichols and Hayasaka, 2003)]. A significant level of corrected $p = 0.05$, cluster volume of 160 mm^3 (corresponds to 160 voxels and 20 voxels for thickness and CBF maps respectively), were used to identify areas with significant prediction. In addition, we also reported maps using a liberal threshold of uncorrected $p = 0.01$ and cluster volume of 160 mm^3 in Supplementary Figure S1. The voxel-wise analyses were performed in the whole cohort and within the a-MCI and NC groups separately.

3. Results

3.1. Psychometric and demographic at baseline

Table 1 shows the baseline demographic and psychometric data for the a-MCI and NC groups. There are no significant differences in age and education between the two groups, but the proportion of male participants is significantly higher in a-MCI group ($\chi^2_1 = 8.1$, $p = 0.004$). As expected, the a-MCI group's MMSE score is significantly lower than NC ($t_{71} = 3.7$, $p < 0.001$). The a-MCI group also performs significantly poorer in a number of psychometric tests, particularly memory tasks, consistent with their amnestic status. We also observed significant difference in recognition memory on the test phase of the scene-encoding task (d'; $t_{60} = 4.3$, $p < 0.001$). Nonetheless, the memory discrimination of the a-MCI group is far from floor suggesting that they were able to perform the task and displayed reasonable effort.

3.2 Longitudinal changes of neuropsychological data and the estimated rate of hippocampal atrophy

As shown in Table 2, the estimated rate of hippocampal atrophy was significantly lower in NC (−0.80 ± 1.0 %/year) compared to a-MCI (−1.68 ± 1.1 %/year, $t_{68} = 3.5$, $p < 0.001$). This result is consistent with the a-MCI group being enriched in individuals with prodromal AD. However, no psychometric longitudinal measure was significantly different between the two groups, likely due to the mildness of impairment and heterogeneity in underlying etiology, as well as confounds in these longitudinal measures due to practice effects, regression to the mean, and intra-individual variability across test sessions.

Author Manuscript Author Manuscript Author Manuscript Author Manuscript

3.3 ROI correlation analyses

Table 3 shows the results of partial correlation analyses for the resting CBF, task CBF and structural measurements with the estimated rate of hippocampal atrophy in the whole cohort, a-MCI and NC separately. Across the whole cohort, only task CBF in hippocampus (r = 0.36, p = 0.005) and none of the resting CBF or structural measurements was significantly correlated with the estimated rate of hippocampal atrophy. A similar result was observed in the a-MCI group alone. Only task CBF in fusiform gyrus demonstrated significant correlation (r = 0.56, p = 0.003). The effect of total gray matter CBF during task showed a trend in both the whole cohort (r = 0.26, p = 0.045) and a-MCI group (r = 0.49, p = 0.012), as did fusiform (r = 0.31, p = 0.018) and parahippocampal gyrus (r = 0.30, p = 0.021) in the whole cohort, but these did not meet significance when correcting for multiple comparisons. None of the resting CBF or structural measurements was significantly associated with the estimated rate of hippocampal atrophy although there were uncorrected trends in hippocampus (r = 0.24, p = 0.048) and parahippocampal gyrus (r = 0.24, p = 0.045) for structural measurements in the whole cohort. Figure 1(A) and (B) show the scatter plots of the estimated annualized hippocampal atrophy rate and the most predictive ROI measures in a-MCI (fusiform gyrus task CBF) groups and the whole cohort (hippocampal task CBF), respectively. No significant correlation was observed in the NC group. Limiting this analysis to only subjects with all three kinds of measurements available yielded similar results.

The two-step, hierarchical linear regression result showed that only the task CBF in fusiform gyrus [β = 0.081 (95% confidence interval: 0.030, 0.133), p = 0.004] and the task CBF in hippocampus [β = 0.042 (95% confidence interval: 0.013, 0.070), p = 0.005] were included in the most predictive models of the a-MCI group (N = 26, $F_{2,23}$ = 5.3, p = 0.013) and the whole cohort (N = 61, $F_{3,57}$ = 7.2, p < 0.001) respectively. None of the resting CBF or structural measurements provided complementary information to the prediction. When using rate of MMSE change as dependent variable, none of the measures was found to demonstrate significant correlation.

3.4 Voxel-wise correlation analyses

To further explore brain areas in which baseline CBF is predictive of the estimated hippocampal atrophy rate, voxel-wise correlation analyses were performed for resting, task CBF and cortical thickness. The results, shown in Figure 2, are consistent with the ROI analysis. CBF measurements during the scene-encoding task demonstrated significant correlation after correction for multiple comparisons in a-MCI (Figure 2-A1) and the whole cohort (Figure 2-A2), with effect in left fusiform gyrus being significant in both analyses. Using a liberal threshold of uncorrected p < 0.01 (Figure 2B), we observed consistent significant effects along the visual pathway, i.e. hippocampus, parahippocampal gyrus, fusiform gyrus, occipital lobe in both a-MCI and the whole cohort. When just examining the NC subjects, only resting CBF in frontal lobe demonstrated significant correlation (Figure 2-A3). Structural measurements (i.e. cortical thickness), did not demonstrate any significant correlation in all the three groups (a-MCI, NC or the whole cohort).

Author Manuscript Author Manuscript Author Manuscript Author Manuscript

4. Discussion

4.1 Task ASL MRI is most sensitive to hippocampal neurodegeneration

Among MRI derived measurements of structure and function, task ASL MRI provided the strongest prediction for the estimated rate of hippocampal atrophy among a-MCI patients, as well as across the entire cohort. This was observed in both the ROI (Table 3) and the voxel-wise analyses (Figure 2). In all cases, measurement of CBF during rest and structural measures provided no prediction in these groups. The value of a task measure for prediction in the current study is consistent with our prior work (Xie et al., 2016), in which we reported that task ASL MRI provides better discrimination of a-MCI patients relative to NC compared to resting ASL MRI in a cross-sectional analysis. We argued previously that this is because the visual scene-encoding memory task operates as a “brain stress test” that enhances group differences. The current results extend this finding by suggesting that this type of functional measure is also sensitive to those individuals most likely to display greater future neurodegeneration. Moreover, the use of a memory-encoding task appeared to accentuate this prediction relative to obtaining CBF measurements during rest or using structural measures of neurodegeneration. Our findings suggest that in prodromal stages of AD, resting states may not fully capture synaptic or other functional alterations associated with early AD pathology.

From the voxelwise analysis, we can see that the strongest effects localize to the hippocampus, parahippocampal gyrus, fusiform gyrus, and beyond to primary visual association areas (Figure 2-B). This most likely reflects the use of a visually-based scene-encoding task. Prior longitudinal fMRI studies, which reported activations more isolated to the hippocampus proper (Miller et al., 2007; O’Brien et al., 2010; Huijbers et al., 2015) or parietal lobe (Petrella et al., 2007; Vannini et al., 2007; Kochan et al., 2011), demonstrated a similar property of selectivity. The ability to target specific region of the brain could be a potential important strength of incorporating task with MRI. While the visual scene encoding task appears to be robust and effective in eliciting functional deficits in MCI patients, future work should examine other types of task paradigms.

An interesting observation is that total gray matter CBF during task was also associated with the estimated rate of hippocampal atrophy in a-MCI patients ($r = 0.49$, $p = 0.012$) and the whole cohort ($r = 0.26$, $p = 0.045$) at a trend level. The relationship between total gray matter CBF measured with ASL MRI and evidence of neurodegeneration has not been previously investigated. This finding may indicate that the visual scene memory-encoding task not only alters CBF in memory-related regions, but also has global effects that are linked to future neurodegeneration in the hippocampus, a central node of the memory network. Since CBF in total gray matter can be quantified with greater precision than CBF within smaller ROI (Chen et al., 2011a), it may be worth examining this measure in future work assessing the predictive value of task activated CBF in a-MCI.

4.2 Functional abnormality may precede macroscopic structural atrophy

As shown in Section 3.3, only task ASL MRI measurements were included in the most predictive model for neurodegeneration, indicating that structural measurements did not

Author Manuscript Author Manuscript Author Manuscript Author Manuscript

provide complementary information in prediction of future hippocampal atrophy. This supports the notion that functional abnormalities may precede structural atrophy in early stages of the disease. The extent of this functional abnormality appears not be as easily detected in the "resting" state as compared to a task condition involving episodic memory, the cognitive domain most likely to be affected in early disease. It is also notable that the present finding is conceptually similar to recent work suggesting that perfusion abnormalities may precede the entire biomarker cascade of AD (Iturria-Medina et al., 2016).

However, the current finding does appear to differ with the results reported in the only other longitudinal ASL study in this population by Chao et al. (Chao et al., 2010). They reported that resting CBF in right precuneus, inferior parietal, middle cingulum and middle frontal were associated with conversion from MCI to AD and structural measurement (i.e. hippocampal volume) provided complementary prediction. The apparent contradictory results could be due to the relative short time interval between the two time points in this study (1.35 ± 0.33 years in this study versus 2.7 ± 1.0 years in (Chao et al., 2010)). Prediction of change over this relatively short interval may limit the sensitivity of resting ASL or volumetric MRI. Also, the discrepancy could be caused by the difference in outcome measures of the two studies, i.e. a clinical outcome vs. hippocampal neurodegeneration.

4.3. Limitations and future work

Several limitations of the current study need to be addressed in future work. First, the follow-up time in the current analysis was relatively short and not long enough to observe strong clinical outcomes. Indeed, we did not observe that any of the imaging measures predicted MMSE change and that cognitive changes between a-MCI and NC adults were not obvious over the follow-up period. Longer follow-up to clinical outcomes will be important in determining the degree to which task ASL MRI allows for identification of clinically meaningful outcomes. That said, the ability to predict the estimated rate of neurodegeneration is of potential significant utility in earlier phase clinical trials to enrich cohorts and allow for reasonably powered proof-of-concept interventions in smaller cohorts. Second, the sample size is also relatively modest and a larger cohort will be needed to validate these findings. Third, while the estimated hippocampal atrophy rate was used as a surrogate of AD neurodegeneration and progression, it is a relatively non-specific measure and other processes may influence it, such as presence of cerebrovascular disease or other neurodegenerative processes. Future work will need to obtain information about the molecular pathology (e.g. amyloid PET) to determine the specificity of the CBF effects to AD pathophysiology. Fourth, the interaction with other risk factors, e.g. cerebrovascular disease and so on, were not investigated in this study and is important to include in future studies of these populations, particularly when considering CBF measurements. Fifth, the a-MCI and NC subjects were sampled from different populations (clinical vs. non-clinical research cohorts), which may potentially confound the results of the current study. However, since we did not directly compare a-MCI with NC, this is less likely to be a significant concern. Finally, using improved ASL MRI methodology (Vidorreta et al., 2017) in future work should further increase it's sensitivity and reliability as a biomarker of regional brain function.

Author Manuscript Author Manuscript Author Manuscript Author Manuscript

5. Conclusions

We demonstrated that regional CBF measured using ASL MRI during a visual scene memory-encoding task predicts neurodegeneration likely due to AD. In comparison, ASL CBF acquired during rest displayed weaker association with the estimated hippocampal atrophy rate, supporting the notion that a cognitive challenge may accentuate functional abnormalities consistent with prior cross-sectional studies (Xu et al., 2007; Xie et al., 2016). Further, the finding that structural MRI measurements did not show strong correlation with evidence of greater neurodegeneration in a-MCI patients nor provide complementary information in prediction supports the hypothesis that functional abnormalities may precede or exceed the degree of structural atrophy in early disease stages. ASL MRI could have important utility in identifying candidates for AD treatment clinical trials likely to display significant progression.

Supplementary Material

Refer to Web version on PubMed Central for supplementary material.

Acknowledgements:

This work was supported by National Institutes of Health (grant numbers R01-AG037376, R01-EB017255, R01-AG040271, P30-AG010124, K23-AG028018, P41-EB015893, R01-AG056014, R01-AG055005).

Grant information:

Grant sponsor: National Institute of Health; Grant numbers: R01-AG037376, R01-EB017255, R01-AG040271, P30-AG010124, K23-AG028018, P41-EB015893, R01-AG056014, R01-AG055005

References

Alsop DC, Detre JA, Grossman M. 2000 Assessment of cerebral blood flow in Alzheimer's disease by spin-labeled magnetic resonance imaging. Ann Neurol 47:93–100. [PubMed: 10632106]

Binnewijzend MAA, Kuijer JPA, Benedictus MR, van der Flier WM, Wink AM, Wattjes MP, van Berckel BNM, Scheltens P, Barkhof F. 2013 Cerebral Blood Flow Measured with 3D Pseudocontinuous Arterial Spin-labeling MR Imaging in Alzheimer Disease and Mild Cognitive Impairment: A Marker for Disease Severity. Radiology 267:221–230. [PubMed: 23238159]

Braak H, Braak E. 1995 Staging of Alzheimer's disease-related neurofibrillary changes. Neurobiol Aging 16:271–278. [PubMed: 7566337]

Chao LL, Buckley ST, Kornak J, Schuff N, Madison C, Yaffe K, Miller BL, Kramer JH, Weiner MW. 2010 ASL perfusion MRI predicts cognitive decline and conversion from MCI to dementia. Alzheimer Dis Assoc Disord 24:19–27. [PubMed: 20220321]

Chen Y, Wang DJJ, Detre JA. 2011a Test-retest reliability of arterial spin labeling with common labeling strategies. J Magn Reson Imaging 33:940–949. [PubMed: 21448961]

Chen Y, Wolk D a, Reddin JS, Korczykowski M, Martinez PM, Musiek ES, Newberg a B, Julin P, Arnold SE, Greenberg JH, Detre J a. 2011b Voxel-level comparison of arterial spin-labeled perfusion MRI and FDG-PET in Alzheimer disease. Neurology 77:1977–85. [PubMed: 22094481]

Chételat G, Landeau B, Eustache F, Mézenge F, Viader F, de la Sayette V, Desgranges B, Baron J-C. 2005 Using voxel-based morphometry to map the structural changes associated with rapid conversion in MCI: A longitudinal MRI study. Neuroimage 27:934–946. [PubMed: 15979341]

Dai W, Garcia D, de Bazelaire C, Alsop DC. 2008 Continuous flow-driven inversion for arterial spin labeling using pulsed radio frequency and gradient fields. Magn Reson Med 60:1488–97. [PubMed: 19025913]

Author Manuscript Author Manuscript Author Manuscript Author Manuscript

Dai W, Lopez OL, Carmichael OT, Becker JT, Kuller LH, Gach HM. 2009 Mild cognitive impairment and alzheimer disease: patterns of altered cerebral blood flow at MR imaging. Radiology 250:856–66. [PubMed: 19164119]

Das SR, Avants BB, Grossman M, Gee JC. 2009 Registration based cortical thickness measurement. Neuroimage 45:867–79. [PubMed: 19150502]

Das SR, Avants BB, Pluta J, Wang H, Suh JW, Weiner MW, Mueller SG, Yushkevich PA. 2012 Measuring longitudinal change in the hippocampal formation from in vivo high-resolution T2-weighted MRI. Neuroimage 60:1266–79. [PubMed: 22306801]

Dickerson B, Wolk D. 2013 Biomarker-based prediction of progression in MCI: comparison of AD signature and hippocampal volume with spinal fluid amyloid-β and tau. Front Aging Neurosci 5:55. [PubMed: 24130528]

Dolui S, Vidorreta M, Wang Z, Nasrallah IM, Alavi A, Wolk DA, Detre JA. 2017a Comparison of PASL, PCASL, and background-suppressed 3D PCASL in mild cognitive impairment. Hum Brain Mapp 38:5260–5273. [PubMed: 28737289]

Dolui S, Wang Z, Shinohara RT, Wolk DA, Detre JA. 2017b Structural Correlation-based Outlier Rejection (SCORE) algorithm for arterial spin labeling time series. J Magn Reson Imaging 45:1786–1797. [PubMed: 27570967]

Eckerström C, Olsson E, Borga M, Ekholm S, Ribbelin S, Rolstad S, Starck G, Edman Å, Wallin A, Malmgren H. 2008 Small baseline volume of left hippocampus is associated with subsequent conversion of MCI into dementia: The Göteborg MCI study. J Neurol Sci 272:48–59. [PubMed: 18571674]

Fernández-Seara MA, Wang J, Wang Z, Korczykowski M, Guenther M, Feinberg DA, Detre JA. 2007 Imaging mesial temporal lobe activation during scene encoding: comparison of fMRI using BOLD and arterial spin labeling. Hum Brain Mapp 28:1391–400. [PubMed: 17525983]

Filippini N, Ebmeier KP, MacIntosh BJ, Trachtenberg AJ, Frisoni GB, Wilcock GK, Beckmann CF, Smith SM, Matthews PM, Mackay CE. 2011 Differential effects of the APOE genotype on brain function across the lifespan. Neuroimage 54:602–10. [PubMed: 20705142]

den Heijer T, van der Lijn F, Koudstaal PJ, Hofman A, van der Lugt A, Krestin GP, Niessen WJ, Breteler MMB. 2010 A 10-year follow-up of hippocampal volume on magnetic resonance imaging in early dementia and cognitive decline. Brain 133:1163–1172. [PubMed: 20375138]

Huijbers W, Mormino EC, Schultz AP, Wigman S, Ward AM, Larvie M, Amariglio RE, Marshall GA, Rentz DM, Johnson KA, Sperling RA. 2015 Amyloid-β deposition in mild cognitive impairment is associated with increased hippocampal activity, atrophy and clinical progression. Brain 138:1023–1035. [PubMed: 25678559]

Iturria-Medina Y, Sotero RC, Toussaint PJ, Mateos-Perez JM, Evans AC, Initiative TADN. 2016 Early role of vascular dysregulation on late-onset Alzheimer's disease based on multifactorial data-driven analysis. Nat Commun 7:11934. [PubMed: 27327500]

Jack CR, Knopman DS, Jagust WJ, Petersen RC, Weiner MW, Aisen PS, Shaw LM, Vemuri P, Wiste HJ, Weigand SD, Lesnick TG, Pankratz VS, Donohue MC, Trojanowski JQ. 2013 Tracking pathophysiological processes in Alzheimer's disease: an updated hypothetical model of dynamic biomarkers. Lancet Neurol 12:207–16. [PubMed: 23332364]

Kochan NA, Breakspear M, Valenzuela M, Slavin MJ, Brodaty H, Wen W, Trollor JN, Turner A, Crawford JD, Sachdev PS. 2011 Cortical Responses to a Graded Working Memory Challenge Predict Functional Decline in Mild Cognitive Impairment. Biol Psychiatry 70:123–130. [PubMed: 21546002]

Leung KK, Bartlett JW, Barnes J, Manning EN, Ourselin S, Fox NC, Alzheimer's Disease Neuroimaging Initiative. 2013 Cerebral atrophy in mild cognitive impairment and Alzheimer disease: Rates and acceleration. Neurology 80:648–654. [PubMed: 23303849]

Mechanic-Hamilton D, Korczykowski M, Yushkevich PA, Lawler K, Pluta J, Glynn S, Tracy JI, Wolf RL, Sperling MR, French JA, Detre JA. 2009 Hippocampal volumetry and functional MRI of memory in temporal lobe epilepsy. Epilepsy Behav 16:128–38. [PubMed: 19674939]

Miller SL, Fenstermacher E, Bates J, Blacker D, Sperling RA, Dickerson BC. 2007 Hippocampal activation in adults with mild cognitive impairment predicts subsequent cognitive decline. J Neurol Neurosurg Psychiatry 79:630–635. [PubMed: 17846109]

Author Manuscript Author Manuscript Author Manuscript Author Manuscript

Mugler JP, Brookeman JR. 1990 Three-dimensional magnetization-prepared rapid gradient-echo imaging (3D MP RAGE). Magn Reson Med 15:152–157. [PubMed: 2374495]

Nichols T, Hayasaka S. 2003 Controlling the familywise error rate in functional neuroimaging: a comparative review. Stat Methods Med Res 12:419–46. [PubMed: 14599004]

O'Brien JL, O'Keefe KM, LaViolette PS, DeLuca AN, Blacker D, Dickerson BC, Sperling RA. 2010 Longitudinal fMRI in elderly reveals loss of hippocampal activation with clinical decline. Neurology 74:1969–1976. [PubMed: 20463288]

Petersen RC. 2004 Mild cognitive impairment as a diagnostic entity. J Intern Med 256:183–94. [PubMed: 15324362]

Petersen RC. 2016 Mild Cognitive Impairment. Contin Lifelong Learn Neurol 22:404–418.

Petersen RC, Doody R, Kurz A, Mohs RC, Morris JC, Rabins P V., Ritchie K, Rossor M, Thal L, Winblad B. 2001 Current Concepts in Mild Cognitive Impairment. Arch Neurol 58:1985. [PubMed: 11735772]

Petersen RC, Roberts RO, Knopman DS, Boeve BF, Geda YE, Ivnik RJ, Smith GE, Jack CR. 2009 Mild cognitive impairment: ten years later. Arch Neurol 66:1447–55. [PubMed: 20008648]

Petrella JR, Prince SE, Wang L, Hellegers C, Doraiswamy PM. 2007 Prognostic Value of Posteromedial Cortex Deactivation in Mild Cognitive Impairment. PLoS One 2:e1104. [PubMed: 17971867]

Petrie EC, Cross DJ, Galasko D, Schellenberg GD, Raskind MA, Peskind ER, Minoshima S. 2009 Preclinical evidence of Alzheimer changes: convergent cerebrospinal fluid biomarker and fluorodeoxyglucose positron emission tomography findings. Arch Neurol 66:632–7. [PubMed: 19433663]

Raichle ME. 1998 Behind the scenes of functional brain imaging: A historical and physiological perspective. Proc Natl Acad Sci 95:765–772. [PubMed: 9448239]

Sevigny J, Chiao P, Bussière T, Weinreb PH, Williams L, Maier M, Dunstan R, Salloway S, Chen T, Ling Y, O'Gorman J, Qian F, Arastu M, Li M, Chollate S, Brennan MS, Quintero-Monzon O, Scannevin RH, Arnold HM, Engber T, Rhodes K, Ferrero J, Hang Y, Mikulskis A, Grimm J, Hock C, Nitsch RM, Sandrock A. 2016 The antibody aducanumab reduces Aβ plaques in Alzheimer's disease. Nature 537:50–56. [PubMed: 27582220]

Sierra-Marcos A 2017 Regional Cerebral Blood Flow in Mild Cognitive Impairment and Alzheimer's Disease Measured with Arterial Spin Labeling Magnetic Resonance Imaging. Int J Alzheimers Dis 2017:5479597. [PubMed: 28573062]

Small SA. 2005 Alzheimer disease, in living color. NatNeurosci 8:404–405.

Smith SM. 2002 Fast robust automated brain extraction. Hum Brain Mapp 17:143–55. [PubMed: 12391568]

Smith SM, Nichols TE. 2009 Threshold-free cluster enhancement: addressing problems of smoothing, threshold dependence and localisation in cluster inference. Neuroimage 44:83–98. [PubMed: 18501637]

Snodgrass JG, Corwin J. 1988 Pragmatics of measuring recognition memory: applications to dementia and amnesia. J Exp Psychol Gen 117:34–50. [PubMed: 2966230]

Toma S 2015 Arterial Spin Labeling May Contribute to the Prediction of Cognitive Deterioration in. 274.

Tzourio-Mazoyer N, Landeau B, Papathanassiou D, Crivello F, Etard O, Delcroix N, Mazoyer B, Joliot M. 2002 Automated anatomical labeling of activations in SPM using a macroscopic anatomical parcellation of the MNI MRI single-subject brain. Neuroimage 15:273–89. [PubMed: 11771995]

Vannini P, Almkvist O, Dierks T, Lehmann C, Wahlund L-O. 2007 Reduced neuronal efficacy in progressive mild cognitive impairment: A prospective fMRI study on visuospatial processing. Psychiatry Res Neuroimaging 156:43–57.

Vidorreta M, Wang Z, Chang YV., Wolk DA, Fernández-Seara MA, Detre JA. 2017 Whole-brain background-suppressed pCASL MRI with 1D-accelerated 3D RARE Stack-Of-Spirals readout. PLoS One 12:e0183762. [PubMed: 28837640]

Wang H, Suh JW, Das SR, Pluta J, Craige C, Yushkevich PA. 2012 Multi-atlas segmentation with joint label fusion. IEEE Trans Pattern Anal Mach Intell 35:611–623. [PubMed: 22732662]

Author Manuscript Author Manuscript Author Manuscript Author Manuscript

Wang Z 2014 Characterizing early Alzheimer's disease and disease progression using hippocampal volume and arterial spin labeling perfusion MRI. J Alzheimer's Dis JAD 42 Suppl 4:S495–502. [PubMed: 25182742]

Wang Z, Aguirre GK, Rao H, Wang J, Fernández-Seara M a, Childress AR, Detre J a. 2008 Empirical optimization of ASL data analysis using an ASL data processing toolbox: ASLtbx. Magn Reson Imaging 26:261–9. [PubMed: 17826940]

Wang Z, Das SR, Xie SX, Arnold SE, Detre J a, Wolk D a. 2013 Arterial spin labeled MRI in prodromal Alzheimer's disease: A multi-site study. NeuroImage Clin 2:630–6. [PubMed: 24179814]

Winblad B, Palmer K, Kivipelto M, Jelic V, Fratiglioni L, Wahlund L-O, Nordberg A, Bäckman L, Albert M, Almkvist O, Arai H, Basun H, Blennow K, de Leon M, DeCarli C, Erkinjuntti T, Giacobini E, Graff C, Hardy J, Jack C, Jorm A, Ritchie K, van Duijn C, Visser P, Petersen RC. 2004 Mild cognitive impairment--beyond controversies, towards a consensus: report of the International Working Group on Mild Cognitive Impairment. J Intern Med 256:240–6. [PubMed: 15324367]

Winkler AM, Ridgway GR, Webster MA, Smith SM, Nichols TE. 2014 Permutation inference for the general linear model. Neuroimage 92:381–97. [PubMed: 24530839]

Wolk DA, Detre JA. 2012 Arterial Spin Labeling MRI: An Emerging Biomarker for Alzheimer's Disease and Other Neurodegenerative Conditions. 25:421–428.

Wu W-C, Fernández-Seara M, Detre JA, Wehrli FW, Wang J. 2007 A theoretical and experimental investigation of the tagging efficiency of pseudocontinuous arterial spin labeling. Magn Reson Med 58:1020–7. [PubMed: 17969096]

Xie L, Dolui S, Das SR, Stockbower GE, Daffner M, Rao H, Yushkevich PA, Detre JA, Wolk DA. 2016 A brain stress test: Cerebral perfusion during memory encoding in mild cognitive impairment. NeuroImage Clin 11:388–397. [PubMed: 27222794]

Xu G, Antuono PG, Jones J, Xu Y, Wu G, Ward D, Li S-J. 2007 Perfusion fMRI detects deficits in regional CBF during memory-encoding tasks in MCI subjects. Neurology 69:1650–6. [PubMed: 17954780]

Author Manuscript Author Manuscript Author Manuscript Author Manuscript

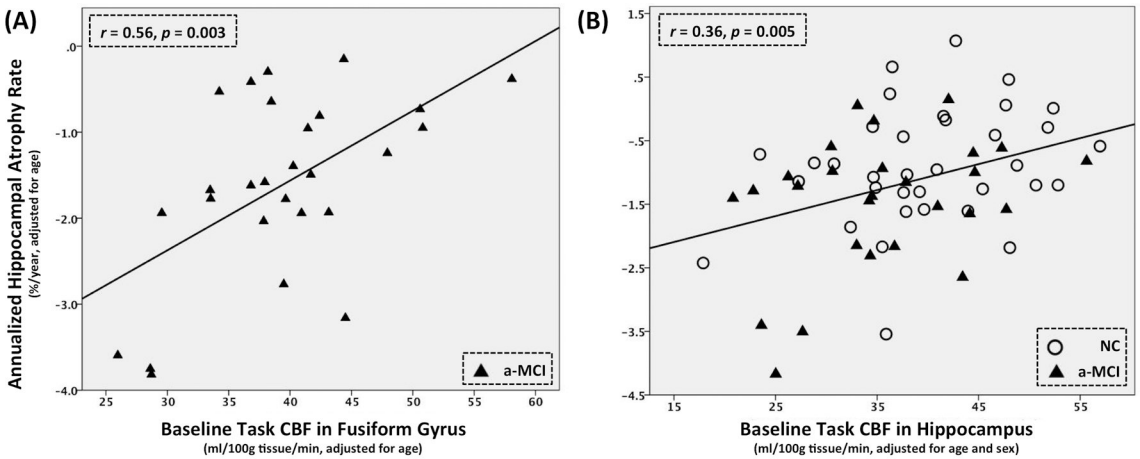

Figure 1.

Scatter plots of the most predictive ROI measures of rate hippocampal atrophy in (A) a-MCI [scene-encoding task CBF (task CBF) in fusiform gyrus] and (B) the whole cohort (task CBF in hippocampus). All measurements are adjusted for age in both plots and sex is an additional covariate for result of the whole cohort in (B). CBF = cerebral blood flow. a-MCI = amnestic mild cognitive impairment. NC = normal control.

Author Manuscript Author Manuscript Author Manuscript Author Manuscript

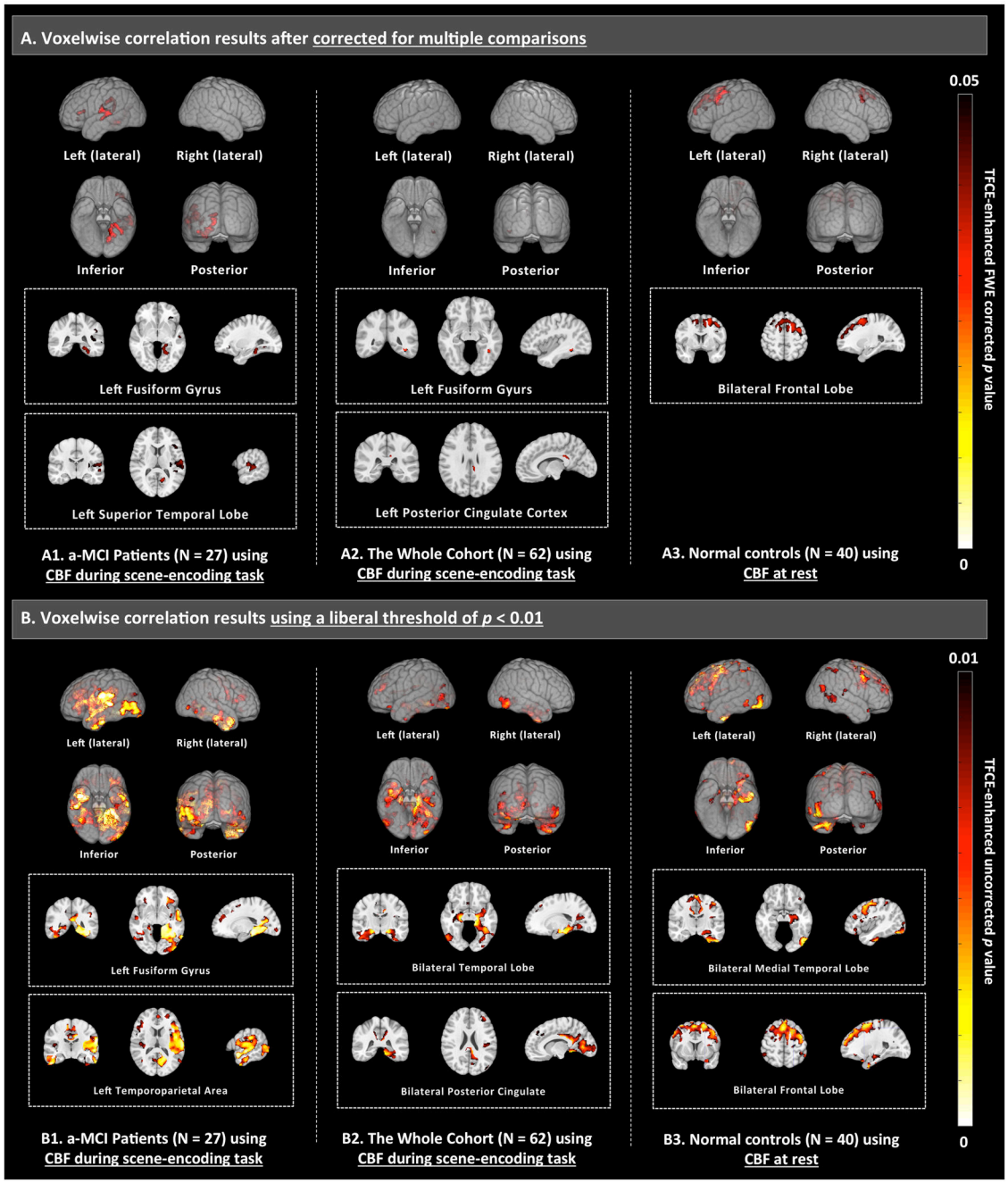

Figure 2.

Voxel-wise correlation between scene-encoding task CBF (task CBF), resting CBF or structural measurements with the estimated rate of hippocampal atrophy, controlling for age (for a-MCI and NC, sex is included as an additional covariate for the whole cohort). The analyses were performed in a-MCI, normal controls and the whole cohort separately. A threshold of family-wise error rate (FWE) corrected $p < 0.05$ and cluster volume of 160 mm^3 (corresponds to 160 voxels and 20 voxels in thickness and CBF maps respectively) were used. Significant effect (shown in the first row) was only observed in resting CBF in normal controls (A3) and task CBF in a-MCI (A1) as well as the whole cohort (A2).

Author Manuscript Author Manuscript Author Manuscript Author Manuscript

Structural measurements, i.e. cortical thickness, did not demonstrate any significant correlation in all the three groups (a-MCI, NC or the whole cohort). In addition, the second row (B) shows the results using a liberal threshold of uncorrected $p < 0.01$. Results of the other measurements using a liberal threshold of uncorrected $p < 0.01$ are shown in Supplementary Figure S1. The effects were shown in 3D glass brain generated using MRIcroGL (top, www.mccauslandcenter.sc.edu/mricrogl) and selected slices (bottom). CBF = cerebral blood flow. TFCE = threshold-free cluster enhancement.

Author Manuscript Author Manuscript Author Manuscript Author Manuscript

Table 1.

Demographic and neuropsychological data

	a-MCI (n=31)		NC (n=42)	
	Mean (STD)	**Range**	**Mean (STD)**	**Range**
Age (years old)	70.9 (6.5)	56 to 83	70.6 (8.8)	55 to 88
Education (years)	16.5 (2.7)	9 to 20	16.3 (3.1)	9 to 20
Female : Male	11 : 20 **	-	29 : 13	-
MMSE	27.8 ** (1.8)	24 to 30	29.1 (1.2)	25 to 30
Trails A (seconds)	37.5 * (14.5)	19 to 69	30.9 (9.8)	18 to 65
Trails B (seconds)	112.3 ** (61.9)	41 to 300	75.4 (28.9)	38 to 161
Digits Forwards Max [a]	6.6 (1.2)	4 to 8	7.0 (1.0)	5 to 8
Digits Backwards Max [a]	4.9 (1.2)	3 to 7	5.1 (1.3)	3 to 7
10-item Word List Immediate Recall	17.8 ** (4.3)	8 to 30	23.5 (3.8)	16 to 30
10-item Word List Delayed Recall	3.6 ** (2.1)	0 to 8	8.0 (2.0)	0 to 10
Category Fluency (animals)	17.6 ** (4.1)	11 to 26	22.0 (5.7)	10 to 31
30-item Boston Naming Test Total	26.8 * (4.0)	19 to 30	28.6 (1.9)	22 to 30
Scene Recognition Memory (d') [b]	1.5 ** (0.9)	−0.5 to 2.9	2.3 (0.6)	1.0 to 3.4

Note: Standard deviations (STD) are in parentheses.

* = $p < 0.05$,

** = $p < 0.01$,

compared to the normal controls, tested by contingency χ^2 test (sex) and independent two-sample t-test (the other items). a-MCI = amnestic mild cognitive impairment. NC = normal control. MMSE = mini mental status examination.

[a] 2 a-MCI patients did not have Digits Forwards and Digits Backwards data available.

[b] 6 a-MCI patients and 5 NC subjects did not have Scene Recognition Memory data available.

Author Manuscript Author Manuscript Author Manuscript Author Manuscript

Table 2.

Longitudinal changes of neuropsychological data and estimated hippocampal atrophy rate

	a-MCI (n=31)		NC (n=42)	
	Mean (STD)	**Range**	**Mean (STD)**	**Range**
MMSE (/year)	−0.53 (1.8)	−2.8 to 6.0	−0.10 (1.3)	−4.9 to 1.9
Trails A (seconds/year) [a]	0.23 (13.0)	−14.5 to 54.1	−0.03 (8.1)	−22.2 to 36.9
Trails B (seconds/year) [a]	7.66 (58.0)	−141.6 to 205.0	3.15 (22.5)	−48.3 to 70.1
Digits Forwards Max (/year) [b]	−0.01 (0.8)	−2.3 to 1.3	−0.01 (0.8)	−2.0 to 1.6
Digits Backwards Max (/year) [b]	−1.1 (1.0)	−2.6 to 2.3	0.08 (0.9)	−2.6 to 1.8
10-item Word List Immediate Recall (/year) [c]	−0.72 (4.7)	−11.3 to 9.6	0.03 (2.8)	−9.2 to 6.1
10-item Word List Delayed Recall (/year) [c]	0.61 (2.4)	−4.5 to 4.2	−0.28 (2.0)	−9.2 to 5.6
Category Fluency (animals) (/year) [c]	−0.93 (4.0)	−8.4 to 10.2	0.57 (2.9)	−5.2 to 7.3
30-item Boston Naming Test Total (/year) [c]	−0.16 (2.3)	−5.5 to 6.3	0.16 (1.2)	−2.5 to 3.8
Estimated Rate of Hippocampal Atrophy (%/year) [d]	−1.68** (1.1)	−3.8 to 0.1	−0.80 (1.0)	−4.2 to 1.5

Note: Negative change indicates the measurement change towards worse condition in the follow-up time point. Standard deviations (STD) are in parentheses.

* = $p < 0.05$,

** = $p < 0.01$, compared to the normal controls, tested by independent two-sample t-tests. Only longitudinal hippocampal atrophy rate, and none of the neuropsychological test result, was significantly different between the two groups. a-MCI = amnestic mild cognitive impairment. NC = normal control. MMSE = mini mental status examination.

[a] 2 a-MCI patients did not have longitudinal Trails A and Trails B data available. 1 additional NC subjects did not have longitudinal Trails B data available.

[b] 3 a-MCI patients and 1 NC subject did not have longitudinal Digits Forwards and Digits Backwards data available.

[c] 1 a-MCI did not have 10-item Word List Immediate/Delayed Recall, Category Fluency (animals) and 30-item Boston Naming Test data available.

[d] 2 a-MCI patients and 1 NC subject were excluded described in Section 2.4.2.

Author Manuscript Author Manuscript Author Manuscript Author Manuscript

Table 3.

Partial correlation between scene-encoding task CBF (task CBF), resting CBF, structural measurements and estimated rate of hippocampal atrophy in a-MCI (controlling for age), normal controls (controlling for age) and the whole cohort (controlling for age and sex). For the whole cohort, sex was included as an additional covariate due to the unmatched sex ratio between a-MCI and normal controls. Significant correlations were highlighted in bold font and the ones survived Bonferroni correlation ($p < 0.05/6$) were highlighted by star signs. 95% confidence intervals were reported in parentheses. Including sex as an additional covariate for within group analyses (a-MCI and normal controls) did not significantly affect the results, shown in Supplementary Table S1. When testing on subjects with all the three kinds of measurements available, the results were similar.

Group	ROI	Task CBF	Resting CBF	Structural Measurements
a-MCI	Number of Subjects	27	28	29
	Gray Matter	***r* = 0.49 (0.11, 0.73)** ***p* = 0.012**	*r* = 0.12 (−0.32, 0.49) *p* = 0.547	*r* = 0.15 (−0.31, 0.54) *p* = 0.454
	Hippocampus	*r* = 0.36 (−0.01, 0.60) *p* = 0.068	*r* = 0.10 (−0.35, 0.37) *p* = 0.962	*r* = 0.07 (−0.25, 0.41) *p* = 0.710
	PCC	*r* = 0.37 (−0.03, 0.71) *p* = 0.063	*r* = 0.15 (−0.35, 0.53) *p* = 0.440	*r* = 0.00 (−0.36, 0.36) *p* = 0.993
	Precuneus	*r* = 0.15 (−0.35, 0.57) *p* = 0.469	*r* = 0.21 (−0.30, 0.60) *p* = 0.300	*r* = −0.09 (−0.47, 0.41) *p* = 0.666
	Fusiform Gyrus	***r* = 0.56 (0.15, 0.77)** ***p* = 0.003***	*r* = 0.06 (−0.38, 0.43) *p* = 0.770	*r* = 0.11 (−0.40, 0.60) *p* = 0.584
	Parahippocampal Gyrus	*r* = 0.33 (−0.07, 0.63) *p* = 0.102	*r* = −0.05 (−0.38, 0.33) *p* = 0.816	r = 0.20 (−0.25, 0.59) *p* = 0.320
Whole Cohort	Number of Subjects	62	68	70
	Gray Matter	***r* = 0.26 (0.07, 0.44)** ***p* = 0.045**	*r* = 0.15 (0.03, 0.31) *p* = 0.233	*r* = 0.00 (−0.23, 0.23) *p* = 0.980
	Hippocampus	***r* = 0.36 (0.15, 0.54)** ***p* = 0.005 ***	*r* = 0.11 (−0.11, 0.31) *p* = 0.386	***r* = 0.24 (0.04, 0.43)** ***p* = 0.048**
	PCC	*r* = 0.19 (0.06, 0.39) *p* = 0.151	*r* = 0.21 (0.01, 0.40) *p* = 0.090	*r* = 0.01 (−0.21, 0.25) *p* = 0.909
	Precuneus	*r* = 0.12 (−0.09, 0.33) *p* = 0.348	*r* = 0.23 (0.01, 0.44) *p* = 0.067	*r* = −0.09 (−0.28, 0.10) *p* = 0.463
	Fusiform Gyrus	***r* = 0.31 (0.08, 0.51)** ***p* = 0.018**	*r* = 0.11 (−0.09, 0.29) *p* = 0.397	*r* = 0.05 (−0.20, 0.31) *p* = 0.679
	Parahippocampal Gyrus	***r* = 0.30 (0.07, 0.51)** ***p* = 0.021**	*r* = 0.08 (−0.13, 0.28) *p* = 0.542	***r* = 0.24 (0.01, 0.47)** ***p* = 0.045**
NC	Number of Subjects	35	40	41
	Gray Matter	*r* = 0.26 (0.02, 0.47) *p* = 0.139	*r* = 0.26 (0.01, 0.48) *p* = 0.103	*r* = −0.31 (−0.53, −1.0) *p* = 0.051
	Hippocampus	*r* = 0.33 (0.02, 0.58) *p* = 0.057	*r* = 0.28 (−0.03, 0.50) *p* = 0.084	*r* = 0.15 (−0.24, 0.48) *p* = 0.356
	PCC	*r* = 0.15 (−0.16, 0.40) *p* = 0.390	*r* = 0.25 (−0.05, 0.50) *p* = 0.118	*r* = −0.10 (−0.38, 0.20) *p* = 0.545
	Precuneus	*r* = 0.17 (−0.09, 0.40) *p* = 0.348	*r* = 0.27 (−0.05, 0.52) *p* = 0.100	*r* = −0.12 (−0.37, 0.11) *p* = 0.446

Author Manuscript

Author Manuscript

Author Manuscript

Author Manuscript

Group	ROI	Task CBF	Resting CBF	Structural Measurements
	Fusiform Gyrus	r = 0.25 (−0.01, 0.49) p = 0.145	r = 0.22 (0.00, 0.41) p = 0.176	r = −0.08 (−0.37, 0.20) p = 0.646
	Parahippocampal Gyrus	r = 0.25 (−0.01, 0.50) p = 0.150	r = 0.25 (0.00, 0.46) p = 0.105	r = −0.01 (−0.36, 0.30) p = 0.956

*
Note: = p < 0.05,

**
= p < 0.01, indicate significant effects after corrected for multiple comparisons. PCC = posterior cingulate cortex. ROI = region of interest. CBF = cerebral blood flow. a-MCI = amnestic mild cognitive impairment. NC = normal control.